The fields from a finite electrical dipole-
A new computational approach

Kurt I. Sørensen* and Niels B. Christensen*

ABSTRACT

Controlled-source, frequency-domain, and time-domain electromagnetic methods require accurate, fast, and reliable methods of computing the electric and magnetic fields from the source configurations used. Except for small magnetic dipole sources, all electric and magnetic sources are composed of lengths of straight wire, which may be grounded. If the source-receiver separation is large enough, the composite electrical dipoles may be considered to be infinitely small, and in a 1-D earth model the fields are expressed as Hankel transforms of an input function, which depends only on the model parameters. The Hankel transforms can be evaluated using the digital filter theory of fast Hankel transforms. However, the approximation of the infinitely small dipole is not always valid, and fields from a finite electrical dipole must be calculated. Traditionally, this is done by numerical integration of the fields from an infinitesimal dipole, thus increasing computation time considerably.

The fields from the finite electrical dipole are expressed as Hankel transforms and as integrals of Hankel transforms. The theory of fast Hankel transforms is extended to include integrals of Hankel transforms, and a method is devised for calculating the filter coefficients. Unlike the fast Hankel transform, the computation involved in the integrated Hankel transforms is not a true convolution, and so a set of filter coefficients must be calculated for each source-receiver configuration. Furthermore, the method is extended to include the calculation of potential differences where one more integration is involved, which is what is actually measured in the field. The computation of filter coefficients is very fast, and for standard configurations, the coefficients need be computed only once. The method is as fast, accurate, and reliable as the fast Hankel transforms method, and is up to an order of magnitude faster than the usual numerical integration.

INTRODUCTION

The theoretical problem of calculating electric and magnetic fields from a grounded electrical dipole of finite length was solved many decades ago (Sommerfeld, 1926; Foster, 1931). The first formulations dealt with the homogeneous half-space model, but expressions for two-layer earths were also found (Riordan and Sunde, 1933; Hohmann, 1973). An extensive study of the responses of a multilayer earth was done by Dey and Morrison (1973), and Wynn and Zonge (1975) and included the effect of anisotropy when calculating the mutual coupling between grounded electrical dipoles. Most of these studies were concerned with calculating inductive coupling present during IP measurements.

It has been suggested (Wynn and Zonge, 1977) that the inductive coupling between the transmitter and receiver dipoles may contain useful information about the earth parameters. This is consistent with the observation that a combination of galvanic and inductive methods in many cases gives a better resolution of earth model parameters than either separately (Jupp and Vozoff, 1975).

The present method of calculating fields from a finite electrical dipole was motivated by the desire to interpret both galvanic and inductive components in geoelectrical soundings. The ac geoelectrical sounding method (Sorensen, 1979; Sorensen et al., 1979; Christensen, 1987; Christensen, 1989) is a combined galvanic/inductive method, where the amplitude of the potential from a finite electrical dipole is measured in a half-Schlumberger electrode configuration (Figure 1) at logarithmically spaced frequencies between 76 and 9765 Hz. The measured total potential difference includes both the galvanic and the inductive fields, so in one

single measuring procedure both galvanic and inductive information is obtained, which gives an enhanced resolution of the conductivity structure of the earth. The measurements are interpreted with a 1-D, plane parallel, and transversely isotropic earth model by means of an automatic, iterative least-squares inversion program. Without the presented method of fast and reliable computations of electric and magnetic fields from a grounded electrical dipole of finite length carrying ac current, the interpretation of ac geoelectrical soundings would be considerably more time consuming.

THE FIELDS FROM A FINITE ELECTRICAL DIPOLE

Numerous papers in the literature have dealt with the derivation of expressions for the fields from a grounded electrical dipole of finite length, and the derivation will not be repeated here. We will depart from the expressions given in Ward and Hohmann (1989) by assuming the dipole to be centered at the origin and extending from $-a$ to a along the x-axis (Figure 2). The expressions for the fields on the surface in a coordinate system with the z-axis positive downwards are

$$E_x(x, y) = \frac{-I}{4\pi} \int_0^\infty \left[(1 - \gamma_{TM}) \frac{u_0}{\hat{y}_0} - (1 + \gamma_{TE}) \frac{\hat{z}_0}{u_0} \right]$$

$$\times \left\{ \frac{x + a}{r^+} J_1(\lambda r^+) - \frac{x - a}{r^-} J_1(\lambda r^-) \right\} d\lambda$$

$$- \frac{I}{4\pi} \int_{-a}^a dx' \int_0^\infty (1 + \gamma_{TE}) \frac{\hat{z}_0}{u_0} \lambda J_0(\lambda r') d\lambda,$$

$$(1)$$

$$E_y(x, y) = \frac{-I}{4\pi} \int_0^\infty \left[(1 - \gamma_{TM}) \frac{u_0}{\hat{y}_0} - (1 + \gamma_{TE}) \frac{\hat{z}_0}{u_0} \right]$$

$$\times \left\{ J_1(\lambda r^+) \frac{y}{r^+} - J_1(\lambda r^-) \frac{y}{r^-} \right\} d\lambda, \qquad (2)$$

$$H_x(x, y) = \frac{I}{4\pi} \int_0^\infty (\gamma_{TM} + \gamma_{TE})$$

$$\times \left\{ J_1(\lambda r^+) \frac{y}{r^+} - J_1(\lambda r^-) \frac{y}{r^-} \right\} d\lambda, \qquad (3)$$

$$H_y(x, y) = \frac{-I}{4\pi} \int_0^\infty (\gamma_{TM} + \gamma_{TE})$$

$$\times \left\{ J_1(\lambda r^+) \frac{x + a}{r^+} - J_1(\lambda r^-) \frac{x - a}{r^-} \right\} d\lambda$$

$$- \frac{I}{4\pi} \int_{-a}^a dx' \int_0^\infty (1 - \gamma_{TE}) \lambda J_0(\lambda r') d\lambda,$$

$$(4)$$

$$H_z(x, y) = \frac{I}{4\pi} \int_{-a}^a \frac{y}{r'} dx' \int_0^\infty (1 + \gamma_{TE}) \frac{\lambda^2}{u_0} J_1(\lambda r') d\lambda,$$

$$(5)$$

w h e r e

$$r^\pm = \sqrt{(x \pm a)^2 + y^2}, \qquad r' = \sqrt{(x - x')^2 + y^2};$$

$$\gamma_{TM} = \gamma_0 \text{ for } q_m = \hat{y}_m, \qquad \gamma_{TE} = \gamma_0 \text{ for } q_m = \hat{z}_m;$$

$$\gamma_m = g_m \frac{\gamma_{m+1} + \psi_{m+1}}{1 + \gamma_{m+1} \psi_{m+1}}, \qquad \gamma_L = 0;$$

$$g_m = \exp\left[-2\alpha_m h_m \right],$$

$$g_0 = 1, \quad h_m: \text{ layer thicknesses};$$

$$\psi_{m+1} = \left(\frac{u_m}{q_m} - \frac{u_{m+1}}{q_{m+1}} \right) \cdot \left(\frac{u_m}{q_m} + \frac{u_{m+1}}{q_{m+1}} \right)^{-1};$$

$$u_m^2 = \lambda^2 - k_m^2,$$

$$k_m^2 = -\hat{z}_m \hat{y}_m = -i\omega\mu_m\sigma_m + \omega^2\mu_m\varepsilon_m;$$

$$\hat{z}_m = i\omega\mu_m, \qquad \hat{y}_m = \sigma_m + i\omega\varepsilon_m;$$
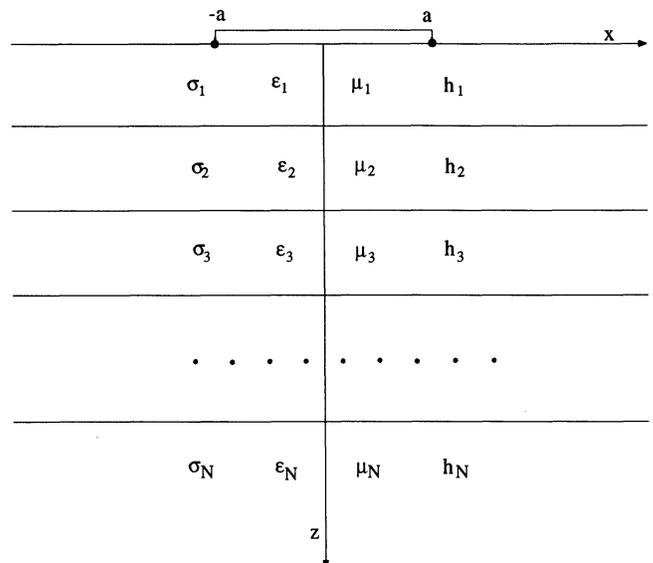
FIG. 2. The source and model configuration. The model parameters σ_m, ε_m, μ_m, and h_m are the conductivity, the dielectric permittivity, the magnetic permeability, and the thickness of the mth layer, respectively. The source is an electrical dipole centered at the origin and extending from $-a$ to a on the x-axis of a right-hand Cartesian coordinate system with the z-axis positive downwards.
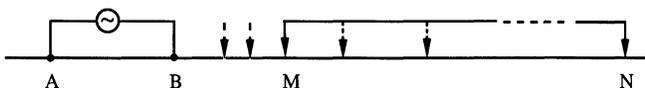
FIG. 1. The half-Schlumberger electrode configuration used in the ac geoelectrical sounding method. A and B are stationary current electrodes; one potential electrode N is placed "far away" and the inner potential electrode M is moved outwards during the sounding. For small transmitter-receiver separations this is essentially a pole-dipole configuration, while for larger transmitter-receiver separations it is a collinear dipole-dipole configuration.

μ_m, ε_m, σ_m, and h_m are the magnetic permeability, the dielectric permittivity, the electric conductivity, and the thickness of the mth layer, respectively. Except for the sign of the first term in equation (4), these are identical to the expressions in Ward and Hohmann (1989).

The expressions for the electric and magnetic fields from a finite electrical dipole are of two different types. One is the ordinary Hankel transform integral

$$\int_0^\infty f(\lambda) J_\nu(\lambda r)\, d\lambda \qquad \nu = 0, 1, \tag{6}$$

which expresses the fields arising from the end points of the dipole. The electric field perpendicular to the dipole E_y and the magnetic field parallel to the dipole H_x are expressed through these integrals alone. The electric field parallel to the dipole E_x and the magnetic field perpendicular to the dipole H_y are expressed through the above Hankel transforms *plus* integrals of Hankel transforms of the type

$$\int_{-a}^a dx' \int_0^\infty f(\lambda) J_\nu(\lambda r')\, d\lambda, \qquad r' = \sqrt{(x-x')^2 + y^2}, \tag{7}$$

which expresses the dependence on the length of wire connecting the grounding points. An integral of the latter type also expresses the vertical magnetic field H_z. The first type can be calculated using the digital filter theory of fast Hankel transforms (Johansen and Sorensen, 1979; Christensen, 1990), while the second type has required a numerical integration. A digital filter theory for the latter type shall be developed in the following paragraphs.

The above observations regarding the dependence of the field components on the endpoints are also given by Kauahikaua (1978), who reaches the same conclusions by comparing field expressions for the finite electrical dipole with fields from an infinitely long straight wire.

THE FILTER THEORY OF INTEGRATED HANKEL TRANSFORMS

From the foregoing paragraphs, we see that the electric and magnetic fields from a finite electrical dipole are expressed as ordinary Hankel transforms or as integrals of Hankel transforms. The Hankel integrals of the type

$$g(r) = \int_0^\infty f(\lambda) J_\nu(\lambda r)\, d\lambda \tag{8}$$

are calculated using the digital filter theory of fast Hankel transforms. This method and the theory behind it are now well established (Johansen and Sorensen, 1979; Anderson, 1989; Christensen, 1990). The input function $f(\lambda)$ is sampled logarithmically and convolved with precalculated filter coefficients, whereby the output function $g(r)$ is obtained at logarithmically distributed sample points.

The parts of the fields expressed as integrals of Hankel transforms of the type

$$g(a, r) = \int_{-a}^a dx' \int_0^\infty f(\lambda) J_\nu(\lambda r')\, d\lambda,$$
$$r' = \sqrt{(x-x')^2 + y^2} \tag{9}$$

have traditionally been calculated by numerical integration of the Hankel transform. However, we shall extend the digital filter theory of fast Hankel transforms to include single and multiple integrals of Hankel transforms. We shall see that integrals like expression (9) can be computed by convolving logarithmically sampled values of the input function $f(\lambda)$ with a set of precalculated filter coefficients, the only difference from the ordinary Hankel transform being that the set of filter coefficients will be dependent on the transmitter-receiver configuration. In this respect it is not a true convolution. As with ordinary fast Hankel transforms, accuracy of the method and speed of operation depend mainly on the analytical properties of the input function $f(\lambda)$, as explained by Johansen and Sorensen (1979) and Christensen (1990).

Reformulation of the problem

Since equation (9) can be rewritten as

$$g(a, r) = \int_0^{x+a} d\rho \int_0^\infty f(\lambda) J_\nu(\lambda r_\rho)\, d\lambda$$
$$- \int_0^{x-a} d\rho \int_0^\infty f(\lambda) J_\nu(\lambda r_\rho)\, d\lambda, \qquad r_\rho^2 = \rho^2 + y^2, \tag{10}$$

we will investigate expressions of the type

$$T(y, c) = \int_0^c d\rho \int_0^\infty f(\lambda) J_\nu(\lambda r_\rho)\, d\lambda, \qquad c > 0. \tag{11}$$

Since expression (9) is equal to

$$\operatorname{sgn}(x+a) \cdot T(y, |x+a|) - \operatorname{sgn}(x-a) \cdot T(y, |x-a|), \tag{12}$$

and since $T(-y, c) = T(y, c)$, it can be assumed that $y > 0$ throughout this section. Equation (11) is reformulated as

$$T(y, c) = \int_0^c d\rho \int_0^\infty f(\lambda) \lambda^{-\mu} \cdot \lambda^\mu J_\nu(\lambda r_\rho)\, d\lambda. \tag{13}$$

Performing the substitutions

$$\lambda = \exp(-u), \qquad r_\rho = \exp(v), \tag{14}$$

and defining new functions

$$F(u) = f[\exp(-u)] \exp[(\mu-1)u],$$
$$H_\nu^\mu(v) = J_\nu[\exp(v)] \exp(\mu v), \tag{15}$$

we have

$$T(y, c) = \int_0^c d\rho \cdot \exp(-\mu v) \int_{-\infty}^{\infty} F(u) H_\nu^\mu(v - u)\, du. \tag{16}$$

Assuming that the Fourier transform $\hat{F}(s)$ of $F(u)$ exists, equation (16) and the convolution theorem (Bracewell, 1965) imply that

$$T(y, c) = \int_{-\infty}^{\infty} \hat{F}(s) \hat{G}_\nu(y, c, s)\, ds, \tag{17}$$

where

$$\hat{G}_\nu(y, c, s) = \int_0^c \exp\left[(i2\pi s - \mu) v\right] d\rho$$

$$\times \int_{-\infty}^{\infty} H_\nu^\mu(u) \exp(-i2\pi s u)\, du. \tag{18}$$

While ν depends on the field component, μ is arbitrary. For the horizontal electric and magnetic fields $\nu = 0$, while for the vertical magnetic field, we must use $\nu = 1$.

Evaluation of $\hat{G}_\nu(y, c, s)$

The integrals involved in equation (18) can be evaluated by use of equation 11.4.16, Abramowitz and Stegun (1970), and equation 3.254.1, Gradshteyn and Ryzhik (1965). Thus

$$\hat{G}_\nu(y, c, s) = \frac{c}{2}\left(\frac{y}{2}\right)^{-\mu} \cdot \hat{G}_\nu^{(1)}(y, c, s), \tag{19}$$

where

$$\hat{G}_\nu^{(1)}(y, c, s) = \left(\frac{y}{2}\right)^{i2\pi s} \frac{\Gamma\left(\dfrac{\nu + 1}{2} + \dfrac{\mu - 1}{2} - i\pi s\right)}{\Gamma\left(\dfrac{\nu + 1}{2} - \dfrac{\mu - 1}{2} + i\pi s\right)}$$

$$\times {}_2F_1\left(\frac{\mu}{2} - i\pi s, \frac{1}{2}; \frac{3}{2}\,\middle|\, -\frac{c^2}{y^2}\right),$$

which when using equations 15.3.8 and 15.3.3, Abramowitz and Stegun (1970), is rewritten as

$$\hat{G}_\nu(y, c, s) = \frac{\sqrt{\pi}}{2}\left(\frac{y}{2}\right)^{1 - \mu} \cdot \hat{G}_\nu^{(2)}(y, s)$$

$$+ \frac{c}{2}\left(\frac{\sqrt{y^2 + c^2}}{2}\right)^{-\mu} \cdot \hat{G}_\nu^{(3)}(y, c, s), \tag{20}$$

where

$$\hat{G}_\nu^{(2)}(y, s) = \left(\frac{y}{2}\right)^{i2\pi s}$$

$$\times \frac{\Gamma\left(\dfrac{\nu + 1}{2} + \dfrac{\mu - 1}{2} - i\pi s\right)\Gamma\left(\dfrac{\mu - 1}{2} - i\pi s\right)}{\Gamma\left(\dfrac{\nu + 1}{2} - \dfrac{\mu - 1}{2} + i\pi s\right)\Gamma\left(\dfrac{\mu}{2} - i\pi s\right)},$$

$$\hat{G}_\nu^{(3)}(y, c, s) = \left(\frac{\sqrt{y^2 + c^2}}{2}\right)^{i2\pi s} \frac{1}{1 - \mu + i2\pi s}$$

$$\times \frac{\Gamma\left(\dfrac{\nu + 1}{2} + \dfrac{\mu - 1}{2} - i\pi s\right)}{\Gamma\left(\dfrac{\nu + 1}{2} - \dfrac{\mu - 1}{2} + i\pi s\right)}$$

$$\times {}_2F_1\left(\frac{\mu}{2} - i\pi s, 1; \frac{\mu + 1}{2} - i\pi s\,\middle|\, \frac{y^2}{y^2 + c^2}\right),$$

where Γ is the complex gamma function, and ${}_2F_1$ is the hypergeometric function.

The expressions (19) and (20) are identical, but (19) will be used for $|c/y| \leq 1/2$ while (20) shall be used for $|c/y| > 1/2$ to ensure numerical stability (see Appendix A). On the axis $y = 0$ we find

$$\hat{G}_\nu(0, c, s) = \left(\frac{c}{2}\right)^{1 - \mu} 1\,\hat{G}_\nu^{(4)}(c, s), \tag{21}$$

where

$$\hat{G}_\nu^{(4)}(c, s) = \left(\frac{c}{2}\right)^{i2\pi s} \frac{1}{1 - \mu + i2\pi s} X \frac{\Gamma\left(\dfrac{\nu+1}{2} + \dfrac{\mu-1}{2} - i\pi s\right)}{\Gamma\left(\dfrac{\nu+1}{2} - \dfrac{\mu-1}{2} + i\pi s\right)}.$$

For $\nu = 0$ we shall choose $\mu = 2$. This choice gives us expressions without unnecessary complications, and gives the same input function $f_E(\lambda)$ for the integrated Hankel integral as for the ordinary Hankel integral. This is seen from

$$F(u) = f[\exp(-u)] \exp[(\mu - 1)u] = \frac{f(\lambda)}{\lambda}, \qquad \mu = 2. \tag{22}$$

Inserting $\nu = 0$ we find for $\hat{G}_0(y, c, s)$ in the case $\mu = 2$:

$$\hat{G}_0(y, c, s) = \frac{2c}{y^2} \cdot \hat{G}_0^{(1)}(y, c, s), \tag{23}$$

where

$$\hat{G}_0^{(1)}(y, c, s) = \left(\frac{y}{2}\right)^{i2\pi s} \frac{\Gamma(1 - i\pi s)}{\Gamma(i\pi s)}$$

$$\times {}_2F_1\left(1 - i\pi s, \frac{1}{2}; \frac{3}{2}\,\middle|\, -\frac{c^2}{y^2}\right);$$

$$\hat{G}_0(y, c, s) = \frac{\sqrt{\pi}}{y} \cdot \hat{G}_0^{(2)}(y, s) + \frac{c}{y^2 + c^2} \cdot \hat{G}_0^{(3)}(y, c, s),$$

where

$$\tag{24}$$

$$\hat{G}_0^{(2)}(y, s) = \left(\frac{y}{2}\right)^{i2\pi s} \frac{\Gamma(\frac{1}{2} - i\pi s)}{\Gamma(i\pi s)},$$

$$\hat{G}_0^{(3)}(y, c, s) = \left(\frac{\sqrt{y^2 + c^2}}{2}\right)^{i2\pi s} \frac{1}{i\pi s - \frac{1}{2}} \frac{\Gamma(1 - i\pi s)}{\Gamma(i\pi s)}$$

$$\times {}_2F_1\left(1 - i\pi s, 1; \frac{3}{2} - i\pi s \left| \frac{y^2}{y^2 + c^2}\right.\right);$$

$$\hat{G}_0(0, c, s) = \frac{1}{c} \cdot \hat{G}_0^{(4)}(s), \qquad (25)$$

where

$$\hat{G}_0^{(4)}(s) = \left(\frac{c}{2}\right)^{i2\pi s} \frac{1}{i\pi s - \frac{1}{2}} \frac{\Gamma(1 - i\pi s)}{\Gamma(i\pi s)}.$$

The discrete formulation

The expression (16) for $T(y, c)$ is not a convolution integral, but has a more complicated functional dependence on y and c. To find an approximation $T^*(y, c)$ to $T(y, c)$, we shall adopt the same approach as in Johansen and Sorensen (1979), Sorensen (1979), and Christensen (1990), and insert an approximation $F^*(u)$ to $F(u)$ in equation (16). Let $F^*(u)$ be a sampled and interpolated version of $F(u)$:

$$F^*(u) = \sum_{-\infty}^{\infty} F(n\Delta)P\left(\frac{u}{\Delta} - n\right), \qquad \Delta = \frac{1}{2s_c}. \quad (26)$$

The computation of $T(y, c)$ involves the spectrum $\hat{F}(s)$. However, the multiplication of $\hat{F}(s)$ by $\Delta\hat{P}(\Delta s)$, the spectrum of the interpolating function, in equation (17) has a negligible influence on the value of $T(y, c)$ if the cut-off frequency s_c is sufficiently high. The asymptotic behavior of the integrand in equation (17) also depends on $\hat{G}_v(y, c, s)$, but in Appendix B, we show how it is controlled mainly by $\hat{F}(s)$.

Substituting equation (26) into (16), we obtain an approximation $T^*(y, c)$ to $T(y, c)$:

$$T^*(y, c) = \sum_{-\infty}^{\infty} F(n\Delta)G_0^*(y, c, n\Delta), \qquad (27)$$

where

$$G_0^*(y, c, n\Delta)$$

$$= \int_{-\infty}^{\infty} \hat{G}_0(y, c, s)\Delta\hat{P}(\Delta s) \exp(-i2\pi s n\Delta) \, ds. \quad (28)$$

Though $T(y, c)$ is not a convolution integral, we have arrived at a convolution-like expression (27) for $T^*(y, c)$. Contrary to the computation of ordinary Hankel transforms where it is necessary to compute only *one* filter, which then gives us all values of the integral through an ordinary convolution, we must now compute a new filter for each (y, c) argument.

Substituting equation (23), (24), and (25) in (28) we get

$$G_0^*(y, c, n\Delta) = \frac{2c}{y^2} \cdot G_0^{*(1)}\left(y, c, \ln\frac{y}{2} - n\Delta\right), \qquad (29)$$

where

$$G_0^{*(1)}(y, c, v) = \int_{-\infty}^{\infty} \frac{\Gamma(1 - i\pi s)}{\Gamma(i\pi s)}$$

$$\times {}_2F_1\left(1 - i\pi s, \frac{1}{2}; \frac{3}{2} \left| -\frac{c^2}{y^2}\right.\right) \Delta\hat{P}(\Delta s) \exp(i2\pi vs) \, ds,$$

$$G_0^*(y, c, n\Delta) = \frac{\sqrt{\pi}}{y} \cdot G_0^{*(2)}\left(\ln\frac{y}{2} - n\Delta\right)$$

$$+ \frac{c}{y^2 + c^2} \cdot G_0^{*(3)}\left(y, c, \ln\frac{\sqrt{y^2 + c^2}}{2} - n\Delta\right), \quad (30)$$

where

$$G_0^{*(2)}(v) = \int_{-\infty}^{\infty} \frac{\Gamma(\frac{1}{2} - i\pi s)}{\Gamma(i\pi s)} \Delta\hat{P}(\Delta s) \exp(i2\pi vs) \, ds,$$

$$G_0^{*(3)}(y, c, v) = \int_{-\infty}^{\infty} \frac{1}{i\pi s - \frac{1}{2}} \frac{\Gamma(1 - i\pi s)}{\Gamma(i\pi s)}$$

$$\times {}_2F_1\left(1 - i\pi s, 1; \frac{3}{2} - i\pi s \left| \frac{y^2}{y^2 + c^2}\right.\right)$$

$$\times \Delta\hat{P}(\Delta s) \exp(i2\pi vs) \, ds,$$

$$G_0^*(0, c, n\Delta) = \frac{1}{c} \cdot G_0^{*(4)}\left(\ln\frac{c}{2} - n\Delta\right), \qquad (31)$$

where

$$G_0^{*(4)}(v) = \int_{-\infty}^{\infty} \frac{1}{i\pi s - \frac{1}{2}} \frac{\Gamma(1 - i\pi s)}{\Gamma(i\pi s)} \Delta\hat{P}(\Delta s) \exp(i2\pi vs) \, ds.$$

The expression involving $G_0^{*(4)}(v)$ is a true convolution since $G_0^{*(4)}(v)$ is independent of y and c. However, the integrand is not expressable in terms of fast Hankel transform filter functions.

It remains to be shown how the filter coefficients $G_0^*(v)$ are calculated. Following the approach in Johansen and Sorensen (1979), Sorensen (1979), and Christensen (1990), G'",(v) shall be calculated as contour integrals in the complex s-plane by summing the residues from the poles of the integrands. In Appendix A, an example demonstrates how filter coefficients for integrated Hankel transforms may be calculated. The properties of the hypergeometric functions involved in the calculations are analyzed, and the questions of convergence and numerical stability are considered.

Error estimation

To obtain an error estimation, we shall proceed along the same lines as in Johansen and Sorensen (1979) and Christensen (1990).

The spectrum $\hat{F}^*(s)$ of the interpolated function $F^*(u)$ is given by

$$\hat{F}^*(s) = \Delta\hat{P}(\Delta s) \sum_{-\infty}^{\infty} \hat{F}\left(s - \frac{n}{\Delta}\right), \qquad (32)$$

and substituting this expression in equation (17), we obtain

$$|T(y, c) - T^*(y, c)|$$

$$< \int_{-\infty}^{\infty} \left| \hat{F}(s) - \Delta\hat{P}(\Delta s) \sum_{-\infty}^{\infty} \hat{F}\left(s - \frac{n}{\Delta}\right) \right| |\hat{G}_0(y, c, s)| \, ds$$

$$= 2 \int_{-\infty}^{\infty} |\hat{F}(s)|[1 - \hat{P}(\Delta s)]|\hat{G}_0(y, c, s)| \, ds, \qquad (33)$$

where results from Johansen and **Sørensen** (1979) regarding the filter function $\hat{P}(s)$ have been used. By applying the spectrum majorization theorem to F(u), we find

$$|\hat{F}(s)| \le K(\omega_0) \cdot \exp\left(-2\pi\omega_0|s|\right), \qquad (34)$$

$$K(\omega_0) = \max_{\omega < \omega_0} \int_0^{\infty} |f(\lambda \exp(\pm i\omega))| \, d\lambda,$$

where $f(\lambda \exp(\pm iw))$ is analytic within the area $|\omega| < \omega_0$. Substituting this majorant for $|\hat{F}(s)|$ in equation (33) we find

$$|T(y, c) - T^*(y, c)| < 2K(\omega_0) \int_{-\infty}^{\infty} \exp\left(-2\pi\omega_0|s|\right)$$

$$\times [1 - \hat{P}(\Delta s)]|\hat{G}_0(y, c, s)| \, ds. \qquad (35)$$

In the theory of fast Hankel transforms, $|\hat{G}_0| = 1$ identically, and the above error integral can be calculated in closed form. In our case, however, it turns out that $|\hat{G}_0|$ increases as a power function for $|s| \to \infty$. In Appendix B the integral in equation (35) is estimated. The results are that the error is of the same order of magnitude as for fast Hankel transforms, and the error decreases exponentially with the sampling density of the discrete convolution. In Christensen (1990) the error expression of fast Hankel transforms is analysed, and it is shown how the parameters of the filter coefficients may be chosen optimally. This theory of optimized fast Hankel transforms can be applied to the filters for integrated Hankel transforms as well.

Filters for potential differences

In practical applications what is measured is the potential difference between two points. We will restrict ourselves to the following two possibilities: the equatorial dipole configuration and the collinear dipole configuration.

In the equatorial dipole configuration, we wish to compute integrals of the following type

$$\int_{-b}^{b} dx \int_{-a}^{a} dx' \int_0^{\infty} f(\lambda)J_\nu(\lambda r') \, d\lambda,$$

$$r' = \sqrt{(x - x')^2 + y^2}, \qquad \nu = 0, \qquad (36)$$

which is rewritten

$$\int_{-b}^{b} dx \left(\int_0^{x+a} d\rho \int_0^{\infty} f(\lambda)J_\nu(\lambda r_\rho) \, d\lambda \right.$$

$$\left. - \int_0^{x-a} d\rho \int_0^{\infty} f(\lambda)J_\nu(\lambda r_\rho) \, d\lambda \right),$$

$$r_\rho = \sqrt{y^2 + \rho^2}, \qquad (37)$$

where the latter expression is valid for $y > 0$ no matter the signofx $\pm a$.

Following the same lines as in the previous sections we see that the integral over x enters only in the function $\hat{G}_\nu(y, c(x), s)$, so using the previous result (19) we have

$$\hat{G}_\nu(y, a, x, s) = \frac{1}{2}\left(\frac{y}{2}\right)^{-\mu}\left(\frac{y}{2}\right)^{i2\pi s}$$

$$\times \frac{\Gamma\left(\dfrac{\nu+1}{2} + \dfrac{\mu-1}{2} - i\pi s\right)}{\Gamma\left(\dfrac{\nu+1}{2} - \dfrac{\mu-1}{2} + i\pi s\right)}$$

$$\times \left\{ (x+a)_2F_1\left(\frac{\mu}{2} - i\pi s, \frac{1}{2}; \frac{3}{2}\middle| \frac{(x+a)^2}{y^2}\right) \right.$$

$$\left. - (x-a)_2F_1\left(\frac{\mu}{2} - i\pi s, \frac{1}{2}; \frac{3}{2}\middle| \frac{(x-a)^2}{y^2}\right) \right\}, \qquad (38)$$

where x enters only in the expression containing the hypergeometric functions in the brackets.

Let us define the integrated function

$$\hat{G}_\nu^i(y, a, b, s) = \int_{-b}^{b} \hat{G}_\nu(y, a, x, s) \, dx. \qquad (39)$$

Evaluating the integral over x we find

$$\int_{-b}^{b} (x+a)_2F_1\left(\frac{\mu}{2} - i\pi s, \frac{1}{2}; \frac{3}{2}\middle| -\frac{(x+a)^2}{y^2}\right) dx$$

$$= (a+b)^2{}_3F_2\left(\frac{\mu}{2} - i\pi s, \frac{1}{2}, 1; \frac{3}{2}, 2\middle| -\frac{(a+b)^2}{y^2}\right) \qquad (40)$$

and a similar expression for the term involving (x - a).

Using the identity

$$z \cdot {}_3F_2(a_1, a_2, 1; b_1, 2|z) = \frac{(b_1 - 1)}{(a_1 - 1)(a_2 - 1)}$$

$$[{}_2F_1(a_1 - 1, a_2 - 1; b_1 - 1|z) - 1] \qquad (41)$$

and substituting in equation (40) we get

$$\hat{G}_\nu^i(y, a, b, s) = \mathcal{G}_\nu(y, a + b, s) - \mathcal{G}_\nu(y, a - b, s), \qquad (42)$$

where

$$\mathcal{G}_\nu(y, c, s) = 2\left(\frac{y}{2}\right)^{2-\mu} \cdot \mathcal{G}_\nu^{(1)}(y, c, s), \qquad (43)$$

where

$$\hat{\mathcal{G}}_\nu^{(1)}(y, c, s)$$

$$= \left(\frac{y}{2}\right)^{i2\pi s} \frac{1}{\frac{\mu}{2} - 1 - i\pi s} \frac{\Gamma\left(\frac{\nu+1}{2} + \frac{\mu-1}{2} - i\pi s\right)}{\Gamma\left(\frac{\nu+1}{2} - \frac{\mu-1}{2} + i\pi s\right)}$$

$$\times {}_2F_1\left(\frac{\mu}{2} - 1 - i\pi s, -\frac{1}{2}; \frac{1}{2}\bigg| -\frac{c^2}{y^2}\right),$$

or by applying equation 15.3.8 and equation 15.3.3, Abramowitz and Stegun (1970)

$$\hat{\mathcal{G}}_\nu(y, c, s) = \sqrt{\pi}|c|\left(\frac{y}{2}\right)^{1-\mu} \cdot \hat{\mathcal{G}}_\nu^{(2)}(s)$$

$$+ \left(\frac{\sqrt{y^2 + c^2}}{2}\right)^{2-\mu} \cdot \hat{\mathcal{G}}_\nu^{(3)}(y, c, s), \quad (44)$$

where

$$\hat{\mathcal{G}}_\nu^{(2)}(s) = \left(\frac{y}{2}\right)^{i2\pi s} \frac{\Gamma\left(\frac{\nu+1}{2} + \frac{\mu-1}{2} - i\pi s\right)\Gamma\left(\frac{\mu-1}{2} - i\pi s\right)}{\Gamma\left(\frac{\nu+1}{2} - \frac{\mu-1}{2} + i\pi s\right)\Gamma\left(\frac{\mu}{2} - i\pi s\right)},$$

$$\hat{\mathcal{G}}_\nu^{(3)}(y, c, s) = \left(\frac{\sqrt{y^2 + c^2}}{2}\right)^{i2\pi s} \frac{1}{\frac{\mu}{2} - 1 - i\pi s}$$

$$\times \frac{1}{\frac{\mu}{2} - \frac{1}{2} - i\pi s} \frac{\Gamma\left(\frac{\nu+1}{2} + \frac{\mu-1}{2} - i\pi s\right)}{\Gamma\left(\frac{\nu+1}{2} - \frac{\mu-1}{2} + i\pi s\right)}$$

$$\times {}_2F_1\left(\frac{\mu}{2} - 1 - i\pi s, 1; \frac{\mu+1}{2} - i\pi s\bigg| \frac{y^2}{y^2 + c^2}\right).$$

The expressions (43) and (44) are identical, but (43) will be used for $|c/y| \le 1/2$ while expression (44) will be used for $|c/y| > 1/2$ to ensure numerical stability. For the same reasons as with the filters for electric fields, we will again choose $\mu = 2$, which for $\nu = 0$ yields the expression

$$\hat{\mathcal{G}}_0(y, c, s) = -2 \cdot \hat{\mathcal{G}}_0^{(1)}(y, c, s), \quad (45)$$

where

$$\hat{\mathcal{G}}_0^{(1)}(y, c, s)$$

$$= \left(\frac{y}{2}\right)^{-i2\pi s} \frac{\Gamma(1 - i\pi s)}{\Gamma(1 + i\pi s)} {}_2F_1\left(-i\pi s, -\frac{1}{2}; \frac{1}{2}\bigg| -\frac{c^2}{y^2}\right);$$

$$\hat{\mathcal{G}}_0(y, c, s) = \frac{2\sqrt{\pi}}{y}|c| \cdot \hat{\mathcal{G}}_0^{(2)}(s) - \hat{\mathcal{G}}_0^{(3)}(y, c, s), \quad (46)$$

where

$$\hat{\mathcal{G}}_0^{(2)}(s) = \left(\frac{y}{2}\right)^{i2\pi s} \frac{\Gamma(\frac{1}{2} - i\pi s)}{\Gamma(i\pi s)},$$

$$\hat{\mathcal{G}}_0^{(3)}(y, c, s) = \left(\frac{\sqrt{y^2 + c^2}}{2}\right)^{i2\pi s} \frac{1}{\frac{1}{2} - i\pi s} \frac{\Gamma(1 - i\pi s)}{\Gamma(1 + i\pi s)}$$

$$\times {}_2F_1\left(-i\pi s, 1; \frac{3}{2} - i\pi s\bigg| \frac{y^2}{y^2 + c^2}\right).$$

The discrete formulation and the error estimation follow exactly the same lines in the case of filters for the electric fields.

In the case of the collinear dipole we shall evaluate integrals of the following type

$$\int_{b_1}^{b_2} dx \int_{-a}^{a} dx' \int_0^\infty f(\lambda)J_\nu[\lambda(x - x')] \, d\lambda,$$

$$b_1, b_2 > a, \quad \nu = 0, \quad (47)$$

which is rewritten

$$\int_{b_1}^{b_2} dx \int_{x-a}^{x+a} d\rho \int_0^\infty f(\lambda)J_\nu(\lambda\rho) \, d\lambda, \quad \rho = x - x'. \quad (48)$$

In the collinear dipole configuration from formula (21), we have

$$\hat{G}_\nu(a, x, s) = 2^{\mu - 1 - i2\pi s} \frac{1}{1 - \mu + i2\pi s}$$

$$\times \frac{\Gamma\left(\frac{\nu+1}{2} + \frac{\mu-1}{2} - i\pi s\right)}{\Gamma\left(\frac{\nu+1}{2} - \frac{\mu-1}{2} + i\pi s\right)}$$

$$\times \{(x + a)^{1 - \mu + i2\pi s} - (x - a)^{1 - \mu + i\pi s}\}. \quad (49)$$

We define the integrated function

$$\hat{G}_\nu^i(a, b_1, b_2, s) = \int_{b_1}^{b_2} \hat{G}_\nu(a, x, s) \, dx. \quad (50)$$

Evaluating the integral over x we find

$$\int_{b_1}^{b_2} \{(x + a)^{1 - \mu + i2\pi s} - (x - a)^{1 - \mu + i2\pi s}\} \, dx$$

$$= \frac{1}{2 - \mu + i2\pi s} \cdot \{(b_2 + a)^{2 - \mu + i2\pi s}$$

$$- (b_2 - a)^{2 - \mu + i2\pi s} - (b_1 + a)^{2 - \mu + i2\pi s}$$

$$+ (b_1 - a)^{2 - \mu + i2\pi s}\} \quad (51)$$

which results in

$$\hat{G}_\nu^i(a, b_1, b_2, s) = \mathcal{G}_\nu(b_2 + a, s) - \mathcal{G}_\nu(b_2 - a, s)$$

$$- \mathcal{G}_\nu(b_1 + a, s) - \mathcal{G}_\nu(b_1 - a, s), \quad (52)$$

where

$$\mathcal{G}_\nu(c, s) = 2\left(\frac{c}{2}\right)^{-\mu + 2} \cdot \mathcal{G}_\nu^{(4)}(c, s), \quad (53)$$

where

$$\mathcal{G}_\nu^{(4)}(c, s) = \left(\frac{c}{2}\right)^{i2\pi s} \frac{1}{2 - \mu + i2\pi s}$$

$$\times \frac{1}{1 - \mu + i2\pi s} \frac{\Gamma\left(\dfrac{\nu + 1}{2} + \dfrac{\mu - 1}{2} - i\pi s\right)}{\Gamma\left(\dfrac{\nu + 1}{2} - \dfrac{\mu - 1}{2} + i\pi s\right)}.$$

The choice $\nu = 0$, $\mu = 2$ gives us the following expression

$$\mathcal{G}_0(c, s) = \mathcal{G}_0^{(4)}(c, s) = \left(\frac{c}{2}\right)^{i2\pi s} \frac{1}{i2\pi s - 1} \frac{\Gamma(1 - i\pi s)}{\Gamma(1 + i\pi s)}.$$
$$(54)$$

The discrete formulation and the error estimation follows exactly the same lines as with the E-filters.

Modification of the ordinary Hankel integrals

It has now been shown that potential differences in the equatorial and collinear dipole configurations can be calculated using the same input function as the one used for the calculation of electric fields, but with application of a different filter. We would like the same thing to be possible with regard to the ordinary Hankel integrals entering in the expressions for the electric fields.

For the expressions containing ordinary Hankel integrals, we find for the potential differences in the equatorial dipole configuration expressions of the following type

$$\int_{-b}^{b} dx \int_0^\infty f(\lambda)\left\{ J_1(\lambda r^+)\frac{x + a}{r^+} - J_1(\lambda r^-)\frac{x - a}{r^-}\right\} d\lambda,$$

$$r^\pm = \sqrt{(x \pm a)^2 + y^2}$$

$$= \int_0^\infty f(\lambda)\left\{ \int_{-b}^{b} \left[J_1(\lambda r^+)\frac{x + a}{r^+} \right. \right.$$

$$\left. \left. - J_1(\lambda r^-)\frac{x - a}{r^-}\right] dx \right\} d\lambda$$

$$= \int_0^\infty f(\lambda)\left\{ -\frac{2}{\lambda}[J_0(\lambda r_a^+) - J_0(\lambda r_a^-)]\right\} d\lambda,$$

$$r_a^\pm = \sqrt{(a \pm b)^2 + y^2}. \quad (55)$$

We see that if we want to leave the input function $f(A)$ untouched, we must be able to calculate filters of the type $1/\lambda\, J_0(\lambda r)$. This is not possible since the integrand involved in the calculation has a singularity on the real axis. However,

for the difference filter in question, this singularity vanishes, and it is thus possible to calculate the difference filter. A special program has been made to perform this difference filter calculation. Besides leaving the input function $f(A)$ untouched, this method removes the numerical instability that could otherwise have been a problem if we subtracted one Hankel filter from the other. Furthermore, the decay of the product of the input function with the filter coefficients in the discrete convolution is faster with the difference filter than would otherwise have been the case.

In the collinear dipole configuration, we must calculate

$$\int_{b_1}^{b_2} dx \int_0^\infty f(\lambda)\{J_1[\lambda(x + a)] - J_1[\lambda(x - a)]\}\, d\lambda$$

$$= \int_0^\infty f(\lambda)\left\{ \int_{b_1}^{b_2} \{J_1[\lambda(x+a)] - J_1[\lambda(x-a)]\}\, dx \right\} d\lambda$$

$$= \int_0^\infty f(\lambda)\left\{ -\frac{1}{\lambda}\{J_0[\lambda(b_2 + a)] - J_0[\lambda(b_2 - a)] \right.$$

$$\left. - J_0[\lambda(b_1 + a)] + J_0[\lambda(b_1 - a)]\}\right\} d\lambda. \quad (56)$$

For this configuration we may calculate the filter as a difference between two of the foregoing difference filters with $y = 0$.

Application of integrated filters

As mentioned in the introduction, the development of the present method of calculating fields from a finite electrical dipole came from the intention to use ac current in geoelectrical soundings. The ac geoelectrical sounding method (Sorensen, 1979; Sorensen et al., 1979; Christensen, 1987; 1989) is a combined galvanic/inductive method, where the amplitude of the potential from a finite electrical dipole is measured in a half-Schlumberger electrode configuration (Figure 1) at logarithmically spaced frequencies between 76 and 9765 Hz. The measured total potential difference includes both the galvanic and the inductive fields, so in one single measuring procedure both galvanic and inductive information is obtained, which gives an enhanced resolution of the conductivity structure of the earth. The measurements are interpreted with a l-D, plane parallel, and transversely isotropic earth model by means of an automatic, iterative least-squares inversion program. The present method of fast and reliable computations of electric and magnetic fields from a grounded electrical dipole of finite length carrying ac current has facilitated the interpretation of ac geoelectrical soundings considerably.

Figure 3 shows model responses from a four-layer model typical of Danish Quatemary deposits for three different frequencies: 76,2441, and 9765 Hz. The electrode configuration is a half-Schlumberger configuration (Figure 1) with a 10 m transmitter dipole and the far potential electrode 400 m from the transmitter. Calculations are made with a spatial data density of 10 per decade in the interval from 1.26 to 3 16 m for a total data set of 25 points. The normalization of the response to apparent resistivity is done using the dc formula. We see that the low frequency of 76 Hz resembles the dc response and that

all responses coincide with the dc response for small transmitter-receiver separations as is expected. For longer transmitter-receiver separations the curves separate.

In the experimental phase of the development of the method, it was not clear which electrode configuration would be the best, and thus programs for the calculation of filters were made very general. Filter programs for the calculation of horizontal electric and magnetic fields anywhere on the surface from a finite electrical dipole were implemented together with programs for the direct calculation of potential differences in the equatorial dipole and the collinear dipole configuration.

Let us turn to a comparison between the direct calculations using integrated Hankel filters and the traditional method of discrete convolution for the Hankel transform followed by numerical integration. As an example we have taken the calculation of the electric field from a dipole of length 10 m in a collinear dipole-dipole configuration. The electric field is calculated at 23 points at distances from 1.26 m to 200 m from the closest current electrode of the source dipole with a density of 10 data points per spatial decade. In both cases, the calculations are performed to a relative accuracy of 10^{-3} of the field values. Programs are written in FORTRAN77 compiled with the Salford FTN77/486 compiler and run on a Compaq SLT 386s/20 with coprocessor (0.143 MFLOP). Figure 4 presents schematically the processes involved in the two approaches.

The method involving numerical integration begins with the calculation of kernel function values followed by a discrete convolution with filter coefficients to give the field values from an infinitesimal dipole in a set of discrete points. Thereafter a numerical integration over the length of the transmitter dipole is performed using a Simpson integration algorithm or something equivalent for each transmitter-receiver separation in which the field value is wanted. The field values used in the integration algorithm are obtained by interpolating the set of discrete points. Generally, the most

time consuming part is the calculation of the kernel function values, the discrete convolution is very fast (appr. 200 complex floating point operations), and the time used for interpolation in the numerical integration algorithm is comparable with the time used for kernel function value computations. The time used for the calculation of kernel function values increases with the number of layers in the model, while the numerical integration lasts equally long for all models.

The direct method using integrated Hankel filters also begins with the calculation of kernel function values. The number of kernel function values is approximately the same as with the ordinary discrete convolution, since the behavior of the integrated Hankel filters asymptotically is the same as for ordinary Hankel filters. Then follows the discrete convolution with integrated Hankel filter coefficients, one for each transmitter-receiver separation. This concludes the calculations. The time-consuming part is the calculation of the kernel function values. The discrete convolutions take little time, requiring approximately 200 fluid number operations per transmitter-receiver separation. Obviously, this procedure is faster than the traditional method.

Figure 5 shows the computation times of the two approaches as a function of the number of layers in the model. For the integrated filters we see an approximate linear increase in computation time with the number of layers in the model. For the numerical integration scheme, different curves show the time needed for the convolution (kernel function calculations plus discrete convolution), the numerical integration time, and the total time. The numerical integration method takes approximately 1 s longer than the technique using integrated Hankel filters for any number of layers. For a half-space model, this is an increase in computation time with a factor of 3; for a five-layer model, the increase is a factor of 2.

In the ac geoelectrical sounding method, the half-Schlumberger electrode configuration is used (Figure 1). This configuration minimizes the direct source-receiver coupling and
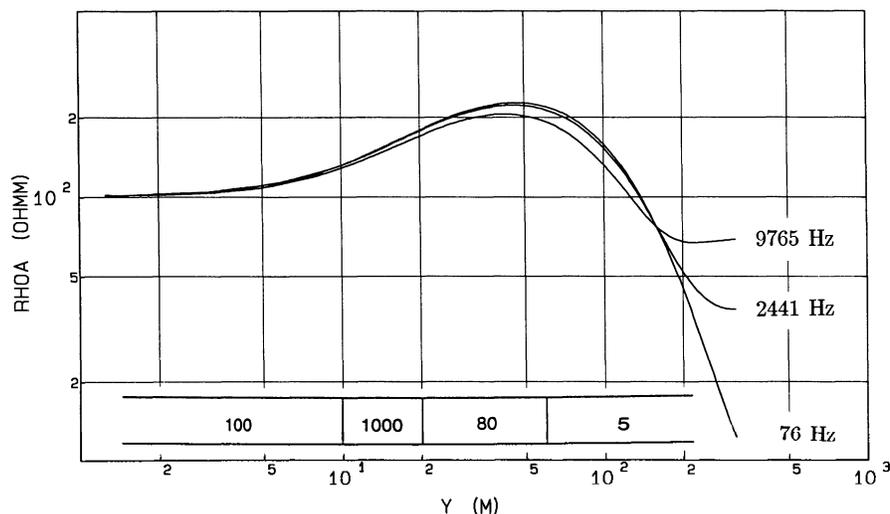

FIG. 3. Four-layer model responses of the ac geoelectrical sounding method. Model curves in the half-Schlumberger electrode configuration for the three frequencies 76, 2441, and 9765 Hz are shown together with the model. The abscissa is the distance between the inner potential electrode and the closest current electrode. The far potential electrode is placed 400 m away, and the source is a 10 m electrical dipole.

the influence from near-surface inhomogeneities, which proved themselves to be major obstacles to unambiguity in the interpretation of a deeper conductivity structure with other electrode configurations. The calculation of the potential differences measured in this configuration takes exactly the same time as the calculation of the fields when the integrated Hankel filters are used. When the potential differences must be calculated by integrating field values numerically, a considerably longer time is needed to integrate over the long receiver dipole. This paper does not deal with the intricacies of two-fold numerical integration, and so no quantitative computation comparisons have been made in the case of potential differences. An estimate is that at least a factor of 10 is gained by the present method of doubly integrated Hankel filters assuming an average number of 10 field values for the integration over the receiver dipole. This is seen from Figure 5, where the interpolation time would increase from approximately 0.8 to 8 s, which is approximately 10 times larger than the average computation time with the integrated filters.

In the practical inversion situation, when measured field data are interpreted with a 1-D earth model, many response calculations are performed, and the differences in computa-tion time add up. Computation time for one iteration equals the number of model parameters plus one times the computation time for a model response. In a four-layer model we have four resistivities, four coefficients of anisotropy, and three layer thicknesses, i.e., one iteration requires 12 responses. Assuming 20 iterations in the inversion procedure, we need 240 response calculations, which equal 3.5 minutes (plus reading and writing) using the integrated Hankel filters. An assumed factor of 10 between the computation times of the two methods means that the numerical integration scheme would take half an hour longer.

RESULTS AND DISCUSSION

In the previous sections, we have demonstrated how it is possible to extend the theory of fast Hankel transforms (Johansen and Sorensen, 1979; Sorensen, 1979; Christensen, 1990) to include the integrals of Hankel transforms appearing in the expressions for electric and horizontal magnetic fields from a finite electrical dipole. The case of the vertical magnetic field, which has not been presented here, can be treated analogously.

Numerical Integration

Calculate input function values

$$\ldots \quad f_{-2} \quad f_{-1} \quad f_0 \quad f_1 \quad f_2 \quad \ldots$$

Convolution with Hankel filter

$$\ldots \quad a_2 f_{-2} + a_1 f_{-1} + a_0 f_0 + a_{-1} f_1 + a_{-2} f_2 \quad \ldots$$

$$\ldots \quad a_2 f_{-1} + a_1 f_0 + a_0 f_1 + a_{-1} f_2 + a_{-2} f_3 \quad \ldots$$

$$\ldots \quad a_2 f_0 + a_1 f_1 + a_0 f_2 + a_{-1} f_3 + a_{-2} f_4 \quad \ldots$$

$$\cdot \quad \cdot \quad \cdot \quad \cdot \quad \cdot \quad \cdot \quad \cdot \quad \cdot \quad \cdot \quad \cdot$$

$$\ldots \quad a_2 f_{m-2} + a_1 f_{m-1} + a_0 f_m + a_{-1} f_{m+1} + a_{-2} f_{m+2}$$
$$\ldots$$

Numerical integration over the source dipole and receiver dipole

Integrated Hankel filters

Calculate input function values

$$\ldots \quad f_{-2} \quad f_{-1} \quad f_0 \quad f_1 \quad f_2 \quad \ldots$$

Convolution with Integrated Hankel filters

$$\ldots \quad a_2^0 f_{-2} + a_1^0 f_{-1} + a_0^0 f_0 + a_{-1}^0 f_1 + a_{-2}^0 f_2 \quad \ldots$$

$$\ldots \quad a_2^1 f_{-2} + a_1^1 f_{-1} + a_0^1 f_0 + a_{-1}^1 f_1 + a_{-2}^1 f_2 \quad \ldots$$

$$\ldots \quad a_2^2 f_{-2} + a_1^2 f_{-1} + a_0^2 f_0 + a_{-1}^2 f_1 + a_{-2}^2 f_2 \quad \ldots$$

$$\cdot \quad \cdot \quad \cdot \quad \cdot \quad \cdot \quad \cdot \quad \cdot \quad \cdot \quad \cdot \quad \cdot$$

$$\ldots \quad a_2^m f_{-2} + a_1^m f_{-1} + a_0^m f_0 + a_{-1}^m f_1 + a_{-2}^m f_2 \quad \ldots$$
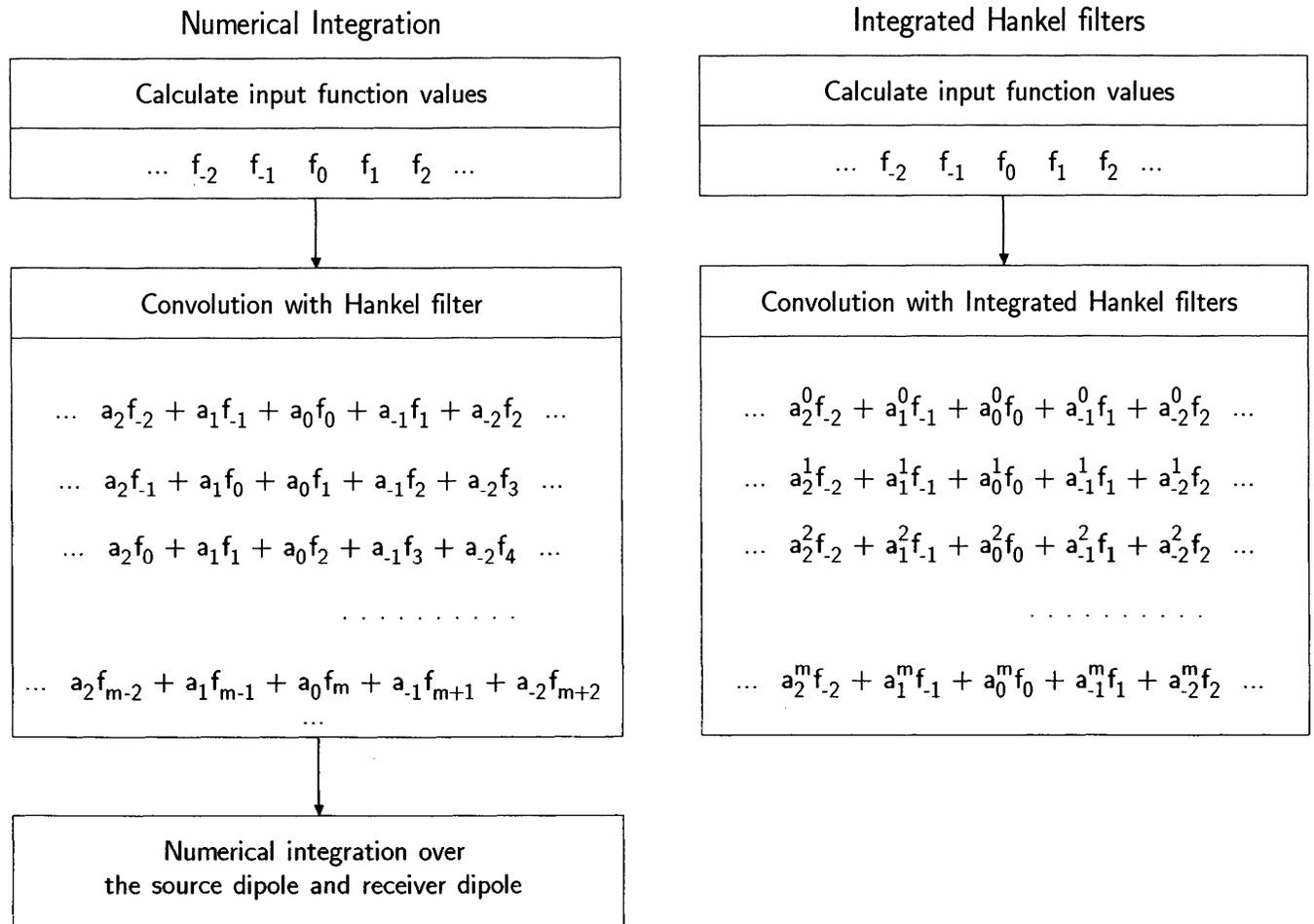
FIG. 4. Schematic presentation of the computational processes involved in the calculation of electric and magnetic fields from the finite electrical dipole using integrated Hankel filters and the ordinary Hankel filters followed by numerical integration, respectively.

Let us turn to an overview of assets and limitations of the new method.

1) The method is elegant. This may in itself not be a conclusive criterion, but it demonstrates the power of analytical work, and it may be an inspiration in other related fields of research.
2) The method possesses all the assets of optimized fast Hankel transforms (Christensen, 1990), which are
   (a) It is possible to estimate the error of the discrete convolution. Though the actual estimations may be difficult to do on paper, it can always be done numerically.
   (b) The error decreases exponentially with the cut-off frequency s_c. This means that a moderate increase in sampling density will make the error decrease dramatically.
   (c) The filter coefficients decrease exponentially for $|v| \to \infty$. This is an important property, since it restricts the discrete convolution to a limited interval.
   (d) The filter coefficients are accurate. The filter coefficients are expressed as series expansions, which makes it possible to evaluate them to any desired accuracy. Thus no additional error in the calculations is introduced from inaccuracies of the filter coefficients.
3) The method is faster. Instead of first performing a discrete convolution between calculated values of the kernel function and precalculated filter coefficients and then numerical integrating, the convolution suffices for the new method presented.
4) Today's increased computer power has brought more time consuming computational tasks within the horizon of ''realizability. '' One aspect is that the computeriza-

tion of data collection has brought a considerable increase in the amount of data measured and thereby in the time needed for their interpretation. Another is that more complicated models for interpretation are used more frequently. Many of these-for example 2- and 3-D modeling-often involve repeated use of 1-D responses, and so the gain in computation time has kept its importance, though it is small for simple applications.

Although a new set of filter coefficients is needed for each transmitter-receiver separation, this is not a serious drawback. In the case of theoretical numerical studies of a particular setup, a set of filter coefficients for a set of distances, which is chosen sufficiently dense for reliable interpolation, is calculated once and for all and used henceforth. In the case of an established field method in an applied electromagnetic method, the same transmitter-receiver configuration is used over and over again, and the pertinent coefficients need only be calculated once and for all, and afterwards, not even interpolation is needed.

If a new set of filter coefficients is demanded, they may be calculated quickly. The filter coefficients may be calculated with the same speed as optimized fast Hankel transform filter coefficients, i.e., approximately 3.5 ms per coefficient plus approximately 500 ms overhead for each transmitter-receiver separation. The filter coefficients are calculated in double precision to a relative accuracy of 10^{-12} (FORTRAN77 programs compiled with the Salford FTN77/486 compiler and run on a Compaq SLT 386s/20 with coprocessor, 0.143 MFLOP).

It is very important to estimate the error of computation. In Appendix B, we demonstrate how the problem of error estimation may be reduced to that known from the theory of optimized fast Hankel transform filters. As mentioned under (2), this error estimation may be difficult in practice with pen and paper, but numerically it is possible. This is in contrast to the method of numerical integration. Although one may use optimized fast Hankel transform filters for the convolution and thus have an error estimate for that part of the computations, it is very difficult to make a reliable error estimation of the numerical integration-and even more difficult for the two-fold numerical integration involved in the calculation of potential differences.

ACKNOWLEDGMENTS

REFERENCES

Abramowitz, M., and Stegun, A. S., 1970, Handbook of mathematical functions: Dover Publ. Inc.
Anderson, W. L., 1989, A hybrid fast Hankel transform algorithm for electromagnetic modeling: Geophysics, 54, 263-266.
Bracewell, R., 1965, The Fourier transform and its applications: McGraw-Hill Book Co.
Christensen, N. B., 1987, The ac-geoelectrical sounding method: a combined electric/electromagnetic prospecting tool: Boreas, 16, 387-392.
- 1989, AC resistivity sounding: First Break, 7, 447-452.
- 1990, Optimized fast Hankel transform filters: Geophys. Prosp., 38, 545-568.
Dey, A., and Morrison, H. F., 1973, Electromagnetic coupling in frequency and time-domain induced polarization surveys over a multilayered earth: Geophysics, 38, 380-405.
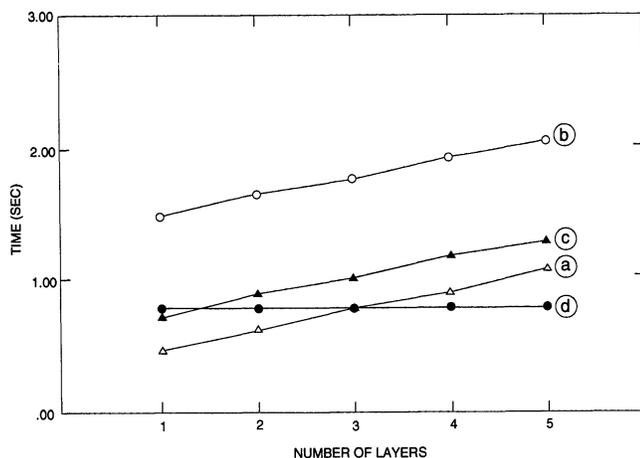

FIG. 5. Comparison of computation times for 23 values of the electric field in the collinear dipole configuration using the integrated Hankel filters and a numerical integration method as a function of the number of layers in the earth model. The curve (a) shows the computation time for integrated Hankel filters; curve (b) shows the computation time for the numerical integration method. The computation time for the numerical integration method consists of the time needed for the convolution shown in curve (c) and the time needed for the numerical integration (d). Thus (b) = (c) + (d).

Foster, R. M., 1931, Mutual impedance of grounded wires lying on the surface of the earth: Bell System Tech. J., 10, 408-419.

Gradshteyn, I. S., and Rhyzik, I. M., 1965, Table of integrals, series, and products, 4th Edition: Academic Press Inc.

Hohmann, G. W., 1973, Electromagnetic coupling between grounded wires at the surface of a two-layer earth: Geophysics, 38, 854-863.

Johansen, H. K., and Sorensen, K., 1979, Fast Hankel transform: Geophys. Prosp., 27, 876-901.

Jupp, D. L. B., and Vozoff, K., 1975, Joint inversion of geophysical data: Geophys. J. Roy. Astr. Soc., 42, 977-991.

Kauahikaua, J., 1978, Electromagnetic fields about a horizontal electric wire source of arbitrary length: Geophysics, 43, 1019-1022.

Riordan, J., and Sunde, E. D., 1933, Mutual impedance of grounded wires for horizontally stratified two-layer earth: Bell System Tech. J., 12, 162.

Sommerfeld, A., 1926, Uber die Ausbreitung der Wellen in der drahtlosen Telegraphie: Annalen der Physik (4), 81, 1135-l 153.

Sorensen, K., 1979, Schlumberger sounding using alternating currents: Ph.D. thesis, University of Aarhus, Denmark.

Sorensen, K., Christensen, N. B., and Jepsen, J. B., 1979, Ac-dc-geoelektrik. Et pilotstudium. (Ac-dc-geoelectrics (A pilot study).) (In Danish): Fredningsstyrelsen, Copenhagen.

Ward, S. H., and Hohmann, G. W., 1989, Electromagnetic theory for geophysical applications, in Nabighian, M. N., Ed., Electromagnetic methods in applied Geophysics: Investigations in geophysics, Vol. 3, Soc. Expl. Geophys., 131-311.

Wynn, J. C., and Zonge, K. L., 1975, EM Coupling, its intrinsic value, its removal and the cultural coupling problem: Geophysics, 40, 83 1-850.

- 1977, Electromagnetic coupling: Geophys. Prosp., 25,29-51.

APPENDIX A

THE CALCULATION OF FILTER COEFFICIENTS

To be able to decide about the convergence of the integral expression for the filter coefficients, we need to find an estimate of the hypergeometric functions involved. Let us first look at the $_2F_1$ function entering in the expressions for the electric field

$$F^{(1)} = {}_2F_1\left(1 - i\pi z, \frac{1}{2}; \frac{3}{2}\middle| -\frac{c^2}{y^2}\right), \quad z = s + i\sigma. \quad (A-1)$$

Equation 15.7.2 Abramowitz and Stegun (1970) gives an asymptotic expansion of $F^{(1)}$

$$|F^{(1)}| \leq \left\{\left|\frac{\Gamma(\frac{3}{2})}{\Gamma(1)}\right|\left|-(1-i\pi z)\frac{c^2}{y^2}\right|^{-1/2} + \frac{\Gamma(\frac{3}{2})}{\Gamma(\frac{1}{2})}\right.$$

$$\times\left|\left|(1-i\pi z)\frac{c^2}{y^2}\right|^{-1}\right|\left|\exp\left[-(1-i\pi z)\frac{c^2}{y^2}\right]\right|\right\}$$

$$\times\left\{1 + \mathbb{O}\left(\left|-(1-i\pi z)\frac{c^2}{y^2}\right|^{-1}\right)\right\}$$

$$\leq\left\{\frac{\sqrt{\pi}}{2}\left|-(1+\pi\sigma)\frac{c^2}{y^2} + i\pi s\frac{c^2}{y^2}\right|^{-1/2}\right.$$

$$+\frac{1}{2}\left|-(1+\pi\sigma)\frac{c^2}{y^2} + i\pi s\frac{c^2}{y^2}\right|^{-1}\exp\left[-(1+\pi\sigma)\frac{c^2}{y^2}\right]\right\}$$

$$\times\left\{1 + \mathbb{O}\left(\left|-(1+\pi\sigma)\frac{c^2}{y^2} + i\pi s\frac{c^2}{y^2}\right|^{-1}\right)\right\}. \quad (A-2)$$

For σ constant, $|s| \to \infty$, we find

$$|F^{(1)}| \sim \frac{y}{2c}\frac{1}{\sqrt{|s|}}, \qquad |s| \to \infty. \quad (A-3)$$

For s constant, $\sigma \to \infty$, we have

$$|F^{(1)}| \sim \frac{y}{2c}\frac{1}{\sqrt{\sigma}}, \qquad \sigma \to \infty, \quad (A-4)$$

while for s constant, $a \to -\infty$, we see that

$$|F^{(1)}| \sim \frac{y^2}{c^2}\frac{1}{2\pi|\sigma|}\exp\left[-(1+\pi\sigma)\frac{c^2}{y^2}\right], \quad \sigma \to -\infty. \quad (A-5)$$

The hypergeometric function thus increases exponentially in the lower complex half-plane, while it decreases slowly in the right, the left, and the upper half-plane.

Let us now consider the $_2F_1$ function entering the expressions for potential differences

$$F^{(2)} = {}_2F_1\left(-i\pi z, -\frac{1}{2}; \frac{1}{2}\middle| -\frac{c^2}{y^2}\right), \quad z = s + i\sigma. \quad (A-6)$$

Equation 15.7.2, Abramowitz and Stegun (1970), gives an asymptotic expansion of $F^{(1)}$

$$|F^{(2)}| \leq \left\{\left|\frac{\Gamma(\frac{1}{2})}{\Gamma(1)}\right|\left|-i\pi z\frac{c^2}{y^2}\right|^{1/2} + \frac{\Gamma(\frac{1}{2})}{\Gamma(-\frac{1}{2})}\left|-i\pi z\frac{c^2}{y^2}\right|^{-1}\right.$$

$$\times\left|\exp\left[-i\pi z\frac{c^2}{y^2}\right]\right|\right\}\left\{1 + \mathbb{O}\left(\left|-i\pi z\frac{c^2}{y^2}\right|^{-1}\right)\right\}$$

$$\leq\left\{\sqrt{\pi}\left|-\pi\sigma\frac{c^2}{y^2} + i\pi s\frac{c^2}{y^2}\right|^{1/2}\right.$$

$$+\frac{1}{2}\left|-\pi\sigma\frac{c^2}{y^2} + i\pi s\frac{c^2}{y^2}\right|^{-1}\exp\left[-\pi\sigma\frac{c^2}{y^2}\right]\right\}$$

$$\times\left\{1 + \mathbb{O}\left(\left|-\pi\sigma\frac{c^2}{y^2} + i\pi s\frac{c^2}{y^2}\right|^{-1}\right)\right\}. \quad (A-7)$$

For σ constant $|s| \to \infty$, we find

$$|F^{(1)}| \sim \frac{\pi c}{y}\sqrt{|s|}, \qquad |s| \to \infty. \quad (A-8)$$

For s constant, $\sigma \to \infty$, we have

$$|F^{(1)}| \sim \frac{\pi c}{y}\sqrt{\sigma}, \qquad \sigma \to \infty, \quad (A-9)$$

while for s constant $\sigma \to -\infty$, we see that

$$|F^{(2)}| \sim \frac{y^2}{2\pi c^2} \frac{1}{|\sigma|} \exp\left[-\pi\sigma \frac{c^2}{y^2}\right], \qquad \sigma \to -\infty. \qquad (A\text{-}10)$$

Thus, the hypergeometric function increases exponentially in the lower complex half-plane, while it increases slowly as a squareroot in the right, the left, and the upper half-plane.

Calculation of the filter coefficients

As an example of how the filter coefficients are calculated let us turn to equation (29). We will show how the expression (29) is found as sums of residues in the complex plane.

We calculate

$$G_0^{*(1)}(y, c, v) = \int_{-\infty}^{\infty} \hat{H}(s)F^{(1)}(y, c, s)\Delta\hat{P}(\Delta s)$$

$$\times \exp(i2\pi v s)\, ds, \qquad (A\text{-}11)$$

where

$$\hat{H}(s) = \frac{\Gamma(1 - i\pi s)}{\Gamma(i\pi s)},$$

$$F^{(1)}(y, c, s) = {}_2F_1\left(1 - i\pi s, \frac{1}{2}; \frac{3}{2}\middle| -\frac{c^2}{y^2}\right),$$

and

$$\hat{P}(s) = \frac{1}{2}\tanh\left[\frac{\pi}{a}\left(s + \frac{1}{2}\right)\right] - \frac{1}{2}\tanh\left[\frac{\pi}{a}\left(s - \frac{1}{2}\right)\right]$$

$$\Delta = \frac{1}{2s_c}.$$

$\hat{H}(\xi), \xi = s + i\sigma$, is analytic except for the points $z_n = -i/\pi$ $(n + 1)$, $n = 0, 1, 2, \ldots$ where it possesses simple poles with the residues

$$R_n = \frac{i(-1)^n}{\pi\Gamma(n + 1)\Gamma(n + 1)}. \qquad (A\text{-}12)$$

$\Delta\hat{P}(\Delta\xi)$ is analytic except for the points $\eta_n^{\pm} = \pm s_c + i2as_c(n + 1/2)$, $n = \ldots -2, -1, 0, 1, 2, \ldots$, where it possesses simple poles with the residues

$$R_n = \mp \frac{a}{2\pi}, \qquad (A\text{-}13)$$

while $F^{(1)}(y, c, s)$ and $\exp(i2\pi v s)$ are analytic everywhere.

Figure A-1 shows the logarithm of the absolute value of the integrand in equation (A-23) seen from a point 10 degrees from the negative imaginary axis towards the positive real axis, and 10 degrees over the complex plane. The poles are given a finite value for clarity. We see the row of poles of $\hat{H}(\xi)$ down the negative imaginary axis and the two rows of poles of $\Delta\hat{P}(\Delta\xi)$.

Consider the contour C_2 of Figure A-2 in the lower half-plane $\xi = s + i\sigma$, $\sigma < 0$. For $\sigma \to -\infty$, $\hat{H}(\xi)$ goes to zero faster than any exponential function, $\Delta\hat{P}(\Delta\xi)$ stays bounded outside its poles, $F^{(1)}(y, c, \xi)$ increases exponentially, and $\exp(i2\pi v \xi)$ decreases exponentially for $v < 0$ and increases exponentially for $v > 0$. Thus the integral along the lower horizontal return path vanishes in the limit for $\sigma \to -\infty$ no matter the sign of v. For σ fixed, $|s| \to \infty$, $\hat{H}(\xi)$ decreases as $|\pi s|^{2\pi\sigma}$ in the lower half-plane, $\exp(i2\pi v\xi)$ stays bounded, $F^{(1)}(y, c, \xi)$ decreases as $|s|^{-1/2}$ and $\Delta\hat{P}(\Delta\xi) \sim \exp(-2\pi/a\,\Delta|s|)$, so the integrals along the vertical paths of C_2 vanish in the limit. We obtain
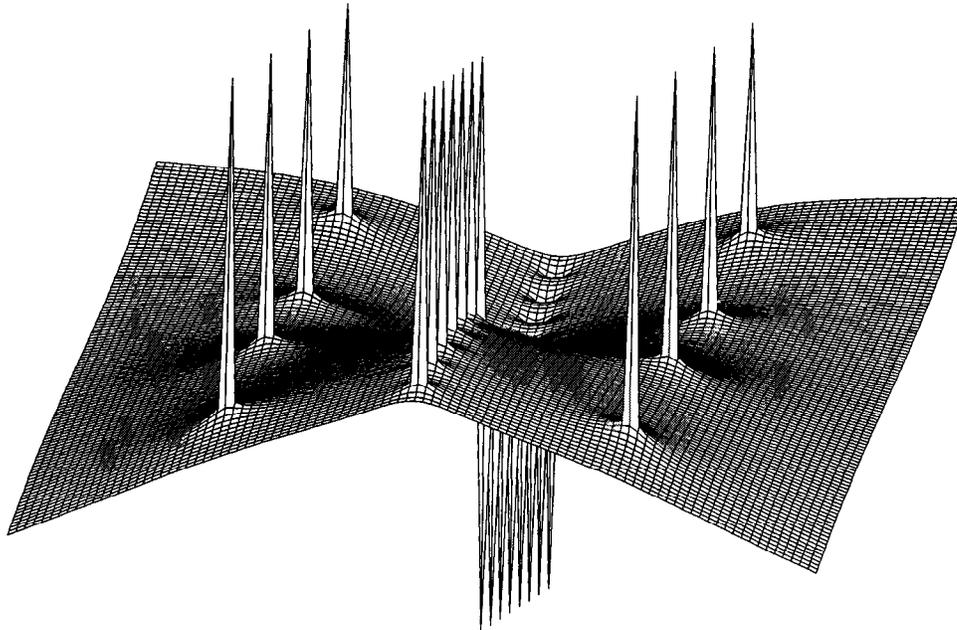
FIG. A-1. The logarithm of the absolute value of the integrand in equation (A-11) for $\omega_0 = (\pi/4)$, $2as_c\omega_0 = 1$ (optimized filters) and $v + (c^2/2x^2) = 0.8$. The surface is seen from a point 10 degrees from the negative imaginary axis towards the positive real axis, and 10 degrees above the complex plane. The poles are given a finite value for clarity. The zeroes of the integrand appear as poles on the positive imaginary axis pointing downward, since the plot is logarithmic.

$$G_0^{*\,(1)}(y, c, v) = -2\pi i \cdot \sum \text{residues inside } C_2$$

$$= -2\pi i \left\{ \sum_{n=0}^{\infty} \frac{i(-1)^n}{\pi \Gamma(n+1)\Gamma(n+1)} \right.$$

$$\times \Delta\hat{P}(\Delta z_n) F^{(1)}(y, c, z_n) \exp(i2\pi v z_n)$$

$$+ \sum_{n=0}^{\infty} -\frac{a}{2\pi} \hat{H}(\eta_n^+) F^{(1)}(y, c, \eta_n^+) \exp(i2\pi v \eta_n^+)$$

$$\left. + \sum_{n=0}^{\infty} \frac{a}{2\pi} \hat{H}(\eta_n^-) F^{(1)}(y, c, \eta_n^-) \exp(i2\pi v \eta_n^-) \right\}.$$

$$(A\text{-}14)$$

Inserting z_n in the exponential function and observing that $\hat{H}(-\bar{\xi}) = \hat{H}(\xi)$ and $F^{(1)}(y, c, -\bar{\xi}) = F^{(1)}(y, c, \xi)$, we find that the second and third sums are each other's conjugates, and we obtain

$$G_0^{*\,(1)}(y, c, v) = \exp(2v) \sum_{n=0}^{\infty} \frac{(-1)^n}{\Gamma(n+1)\Gamma(n+1)}$$

$$\times \exp(2nv) \Delta\hat{P}(\Delta z_n) F^{(1)}(y, c, z_n)$$

$$- 2a \exp(2\pi a s_c v) \text{ Im} \left\{ \exp(i2\pi s_c v) \right.$$

$$\left. \times \sum_{0}^{\infty} \exp(4\pi a s_c n v) \hat{H}(\eta_n^+) F^{(1)}(y, c, \eta_n^+) \right\}. \qquad (A\text{-}15)$$

Though the expression (A-15) is convergent for all values of v, y, and c, we shall only use it for values of $v < v^-$, since for large values of v the first terms of the summation will consist of large alternating terms, and numerical accuracy may be lost. This is accentuated by the presence of the hypergeometric function, since it will contribute to the exponentially increasing terms. Inserting z_n in the asymptotic expansion of $F^{(1)}(y, c, s)$, we see that the exponentially increasing terms of the first sum are proportional to

$$\sim \exp\left(2v + \frac{c^2}{y^2}\right)n. \qquad (A\text{-}16)$$

By demanding $v < v^- = -c^2/2y^2$, we are sure to retain numerical accuracy.

Now, consider the contour C_1 of Figure A-2 encircling the upper half-plane $\xi = s + i\sigma$, $\sigma > 0$. For $\sigma \to \infty$, $\hat{H}(\xi)$ goes to infinity faster than any exponential function, $\Delta\hat{P}(\Delta\xi)$ stays bounded outside its poles, $F^{(1)}(y, c, \xi)$ decreases as $|\sigma|^{-1/2}$, and $\exp(i2\pi v\xi)$ increases exponentially for $v < 0$ and decreases exponentially for $v > 0$. Though $\hat{H}(\xi)$ increases faster than any exponential function, the exponential decay of $\exp(i2\pi v\xi)$ for $v > 0$ introduces a "valley" in which we may place the horizontal return path in the upper half-plane. The minimum in the valley decreases as v increases, so a certain v + exists such that the integral through the valley becomes negligible for $v > v^+$. For σ fixed, $|s| \to \infty$, $\hat{H}(\xi)$ increases as $|\pi s|^{2\pi\sigma}$ in the upper half-plane, $F^{(1)}(y, c, \xi)$ decreases as $|s|^{-1/2}$, $\exp(i2\pi vs)$ stays bounded, and

$\Delta\hat{P}(\Delta\xi) \sim \exp(-2\pi|s|/2as_c)$, and so the integrals along the vertical paths of C_1 vanish in the limit. We obtain

$$G_0^{*\,(1)}(y, c, v) = 2\pi i \, 1 \sum \text{residues inside } C_1$$

$$= 2\pi i \cdot \left\{ \sum_{n=0}^{\infty} -\frac{a}{2\pi} \hat{H}(\eta_n^+) F^{(1)}(y, c, \eta_n^+) \exp(i2\pi v \eta_n^+) \right.$$

$$\left. + \sum_{n=0}^{\infty} \frac{a}{2\pi} \hat{H}(\eta_n^-) F^{(1)}(y, c, \eta_n^-) \exp(i2\pi v \eta_n^-) \right\}, \qquad (A\text{-}17)$$

where $\eta_n^\pm = \pm s_c + i2as_c(n + 1/2)$.

Again we observe that the two sums are each other's conjugates and we obtain

$$G_0^{*\,(1)}(y, c, v) = 2a \exp(-2\pi a s_c v)$$

$$\times \text{Im} \left\{ \exp(i2\pi s_c v) \sum_{n=0}^{N} \exp(-4\pi a s_c n v) \right.$$

$$\left. \times \hat{H}(\eta_n^+) F^{(1)}(y, c, \eta_n^+) \right\}. \qquad (A\text{-}18)$$

For $v^- < v < v^+$ $G_0^{*\,(1)}(y, c, v)$ can be expressed as a discrete Fourier sum minus sums of filter coefficients of arguments to the left and right of v (Christensen, 1990)
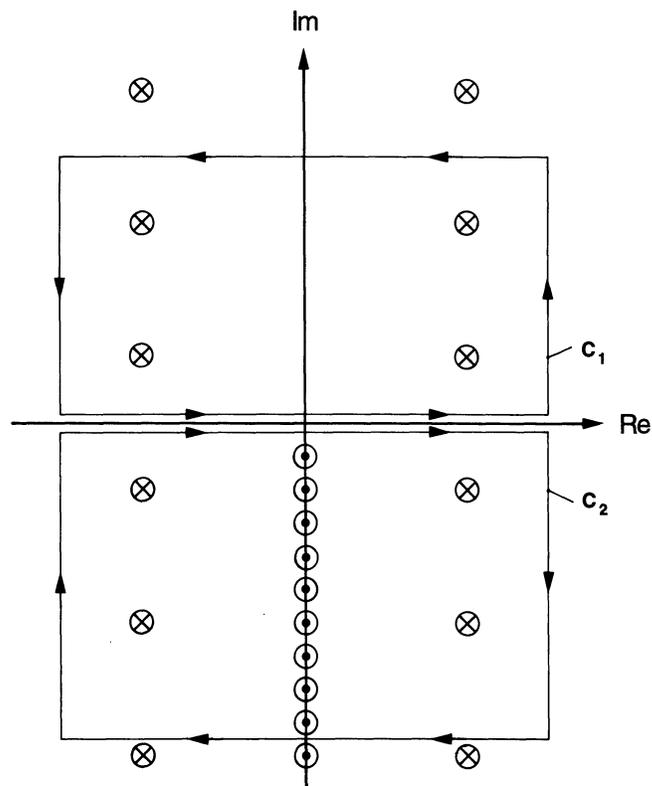

FIG. A-2. The position of the poles of the integrand in equation (A-11) and the integration paths C_1 and C_2 used for the calculation of the filter coefficients. The poles on the negative imaginary axis marked with a circle with a dot belong to the gamma function quotient, the two rows of poles marked with circles with a cross belong to the filter function B(s).

$$G_0^{*\,(1)}(y, c, v) = \Delta_1 \sum_{-\infty}^{\infty} \Delta \hat{P}(n\Delta\Delta_1) \hat{H}(n\Delta_1)$$

$$\times F^{(1)}(y, c, n\Delta_1) \exp(i2\pi v n\Delta_1)$$

$$- \sum_{n=1}^{\infty} G_0^{*\,(1)}\left(y, c, v - \frac{n}{\Delta_1}\right)$$

$$- \sum_{n=1}^{\infty} G_0^{*\,(1)}\left(y, c, v + \frac{n}{\Delta_1}\right). \qquad \text{(A-19)}$$

Choosing Δ_1 so small that $v - 1/\Delta_1 < v^-$ and $v + 1/\Delta_1 > v^+$ for all $v^- < v < v^+$, equation (A-19) enables us to calculate $G_0^{*\,(1)}(y, c, v)$ in the range $v^- < v < v^+$. Here, $1/\Delta_1 = (v^+ - v^-)$ is the greatest Δ_1 meeting this demand and is thus the best one, as a smaller Δ_1 would result in a denser sampling on the real axis of $\Delta \hat{P}(\Delta s) \hat{H}_v(s) F^{(1)}(y, c, s)$.

Except for the presence of the hypergeometric function, the method outlined above is identical with the one for optimized fast Hankel transforms (Christensen, 1990). In the theory of optimized fast Hankel transforms we chose $v^- = 0$ and $v^+ = 4 + 0.1s_c$, but the presence of the hypergeometric function "steals" some of the lower range, which is not "paid back" in the upper range, because it does not decrease exponentially in the upper complex half-plane. Thus the middle range can become very large for c^2/y^2 large, which means that the Fourier sum in the middle range needs a very dense sampling and therefore consists of many terms and numerical accuracy is lost. Therefore, we will choose $v^- = 0$ and restrict ourselves to

$c^2/y^2 < 1/4$, and for $c^2/y^2 > 1/4$ we will use the expression (30)

The method of calculating the filter coefficients in the case of equation (30) and equation (31) is similar in concept to the previous section. In the case of equation (30), we observe that the first term is covered by the theory of fast Hankel transforms. The second term includes the function $1/(i\pi s - 1/2)$, which has a single simple pole on the negative imaginary axis and a hypergeometric function, which has a row of simple poles on the negative imaginary axis. The case of equation (3 1), y = 0, is really just a special case of the second term in equation (30).

Filter coefficients for the calculation of potential differences are computed in an analogous way.

In all cases, the number of residues to be added is quite small. Experience has shown that on the negative imaginary axis and on the lines $|s| = s_c$ less than 20 residues are needed to calculate the sums to a relative accuracy of 10^{-12}. On the real axis less than 100 terms in the Fourier sum are needed.

Computation time is approximately 0.5 ms per coefficient per 1 MFLOP computing power plus approximately 70 ms overhead per 1 MFLOP for each transmitter-receiver separation. A set of 100 filter coefficients can thus be calculated in approximately 120 ms. The filter coefficients are calculated in double precision to a relative accuracy of 10^{-12} using a FORTRAN77 program compiled with a Salford FTN77/486 compiler. Programs for the calculation of filter coefficients for horizontal electric and magnetic fields from a horizontal finite electrical dipole and for potential differences in the equatorial and the collinear dipole-dipole configuration have been made, but filters for the vertical magnetic field have not yet been implemented.

APPENDIX B
ERROR ESTIMATES

In this Appendix we estimate the error integral appearing in the expression (35)

$$|T(y, c) - T^*(y, c)| < 2K(\omega_0) \int_{-\infty}^{\infty}$$

$$\times \exp(-2\pi\omega_0|s|)[1 - \hat{P}(\Delta s)]|\hat{G}_0(y, c, s)|\, ds. \quad \text{(B-1)}$$

In the theory of fast Hankel transforms for ordinary Hankel integrals (Johansen and Sorensen (1979), Christensen, 1990)), we meet an error expression similar to equation (B-1) but with $|\hat{G}_0(y, c, s)| = 1$.

The task is to find majorants for the function $|\hat{G}_0(y, c, s)|$ entering in the filters for the fields and for $|\hat{G}_0(y, c, s)|$ pertaining to the filters for potential differences on the real axis, Im (s) = 0. We will do this for the cases (1):$|c| \le y/2$, (2):$|c| > y/2$, and (3):$y = 0$ mentioned earlier. However, as the expression (2) is identical to (1) for all values of y and c, and the choice between the two expressions is concerned with numerical considerations only, we shall look at the expression (2) for $c \ne 0$ and use (1) for c = 0. On the axis, $y = 0$, we will use the expressions (3). Recalling equation (24), we have

$$\hat{G}_0(y, c, s) = \frac{\sqrt{\pi}}{y}\left(\frac{y}{2}\right)^{i2\pi s} \frac{\Gamma(\frac{1}{2} - i\pi s)}{\Gamma(i\pi s)}$$

$$+ \frac{c}{y^2 + c^2}\left(\frac{\sqrt{y^2 + c^2}}{2}\right)^{i2\pi s} \frac{1}{i\pi s - \frac{1}{2}} \frac{\Gamma(1 - i\pi s)}{\Gamma(i\pi s)}$$

$$\times {}_2F_1\left(1 - i\pi s, 1; \frac{3}{2} - i\pi s \,\middle|\, \frac{y^2}{y^2 + c^2}\right), \qquad \text{(B-2)}$$

and we find

$$|\hat{G}_0(y, c, s)| \le \frac{\sqrt{\pi}}{y}\left|\frac{\Gamma(\frac{1}{2} - i\pi s)}{\Gamma(i\pi s)}\right|$$

$$+ \frac{|c|}{y^2 + c^2}\left|\frac{i\pi s}{i\pi s - \frac{1}{2}}\right|\left|\frac{\Gamma(1 - i\pi s)}{\Gamma(1 + i\pi s)}\right|$$

$$\times \left|{}_2F_1\left(1 - i\pi s, 1; \frac{3}{2} - i\pi s \,\middle|\, \frac{y^2}{y^2 + c^2}\right)\right|$$

$$\leq \frac{\pi}{y} \sqrt{s \tanh \pi^2 s} + \frac{|c|}{y^2 + c^2}$$

$$\times \left| {}_2F_1\left(1 - i\pi s, 1; \frac{3}{2} - i\pi s \left| \frac{y^2}{y^2 + c^2}\right.\right) \right|$$

$$\leq \frac{\pi}{y} \sqrt{s \tanh \pi^2 s} + \frac{|c|}{y^2 + c^2}$$

$$\times \sum_{k=0}^{\infty} \left| \frac{(1 - i\pi s)_k (1)_k}{(\frac{3}{2} - i\pi s)_k (1)_k} \left(\frac{y^2}{y^2 + c^2}\right)^k \right|$$

$$\leq \frac{\pi}{y} \sqrt{s \tanh \pi^2 s} + \frac{|c|}{y^2 + c^2} \sum_{k=0}^{\infty} \left| \left(\frac{y^2}{y^2 + c^2}\right)^k \right|$$

$$\leq \frac{\pi}{y} \sqrt{|s|} + \frac{1}{|c|}. \tag{B-3}$$

This estimate is not valid for c = 0. However, for c = 0 we will investigate the expression, equation (23)

$$\hat{G}_0(y, c, s) = \frac{2c}{y^2} \left(\frac{y}{2}\right)^{i2\pi s} \frac{\Gamma(1 - i\pi s)}{\Gamma(i\pi s)}$$

$$\times {}_2F_1\left(1 - i\pi s, \frac{1}{2}; \frac{3}{2} \left| -\frac{c^2}{y^2}\right.\right), \tag{B-4}$$

and we find

$$|\hat{G}_0(y, 0, s)| = 0, \tag{B-5}$$

which of course is another way of saying that there is no contribution to the field from this term. On the axis y = 0, we will use the expressions (25)

$$\hat{G}_0(c, s) = \frac{1}{c} \left(\frac{c}{2}\right)^{i2\pi s} \frac{1}{i\pi s - \frac{1}{2}} \frac{\Gamma(1 - i\pi s)}{\Gamma(i\pi s)}, \tag{B-6}$$

and we find

$$|\hat{G}_0(c, s)| = \frac{1}{|c|} \left| \frac{1}{i\pi s - \frac{1}{2}} \right| \left| \frac{\Gamma(1 - i\pi s)}{\Gamma(i\pi s)} \right|$$

$$\leq \frac{1}{|c|} \left| \frac{i\pi s}{i\pi s - \frac{1}{2}} \right| \left| \frac{\Gamma(1 - i\pi s)}{\Gamma(1 + i\pi s)} \right| \leq \frac{1}{|c|}. \tag{B-7}$$

Let us turn to the filters for potential differences. Again we use the expression (46) in our estimates. Recalling formula (46)

$$\hat{\mathcal{G}}_0(y, c, s) = \frac{2\sqrt{\pi}}{y} |c| \left(\frac{y}{2}\right)^{i2\pi s} \frac{\Gamma(\frac{1}{2} - i\pi s)}{\Gamma(i\pi s)}$$

$$+ \left(\frac{\sqrt{y^2 + c^2}}{2}\right)^{i2\pi s} \frac{1}{-\frac{1}{2} + i\pi s} \frac{\Gamma(1 - i\pi s)}{\Gamma(1 + i\pi s)}$$

$$\times {}_2F_1\left(-i\pi s, 1; \frac{3}{2} - i\pi s \left| \frac{y^2}{y^2 + c^2}\right.\right), \tag{B-8}$$

we find

$$|\hat{\mathcal{G}}_0(y, c, s)| \leq \frac{2\sqrt{\pi}}{y} |c| \left| \frac{\Gamma(\frac{1}{2} - i\pi s)}{\Gamma(i\pi s)} \right|$$

$$+ \left| \frac{1}{-\frac{1}{2} + i\pi s} \right| \left| \frac{\Gamma(1 - i\pi s)}{\Gamma(1 + i\pi s)} \right|$$

$$\times \left| {}_2F_1\left(-i\pi s, 1; \frac{3}{2} - i\pi s \left| \frac{y^2}{y^2 + c^2}\right.\right) \right|$$

$$\leq \frac{2\pi|c|}{y} \sqrt{s \tanh \pi^2 s}$$

$$+ \sum_{k=0}^{\infty} \left| \frac{(-i\pi s)_k (1)_k}{(\frac{3}{2} - i\pi s)_k} \frac{1}{-\frac{1}{2} + i\pi s} \left(\frac{y^2}{y^2 + c^2}\right)^k \right|$$

$$\leq \frac{2\pi|c|}{y} \sqrt{s \tanh \pi^2 s}$$

$$+ \sum_{k=0}^{\infty} \left| \frac{(1 - i\pi s)_k}{(\frac{3}{2} - i\pi s)_k} \frac{-i\pi s}{(-\frac{1}{2} + i\pi s)(-i\pi s + k)} \left(\frac{y^2}{y^2 + c^2}\right)^k \right|. \tag{B-9}$$

However,

$$\left| \frac{-i\pi s}{(-\frac{1}{2} + i\pi s)(-i\pi s + k)} \right| = \sqrt{\frac{(\pi s)^2}{[\frac{1}{4} + (\pi s)^2][k^2 + (\pi s)^2]}}$$

$$\leq \frac{2}{1 + 2k}. \tag{B-10}$$

Hence from equation 1.643.2, Gradshteyn and Ryzhik (1965)

$$|\hat{\mathcal{G}}_0(y, c, s)|$$

$$\leq \frac{2\pi|c|}{y} \sqrt{s \tanh \pi^2 s} + 2 \sum_{k=0}^{\infty} \frac{1}{1 + 2k} \left(\frac{y^2}{y^2 + c^2}\right)^k$$

$$\leq \frac{2\pi|c|}{y} \sqrt{|s|} + 2 \frac{\sqrt{y^2 + c^2}}{y} \text{Artanh} \frac{y}{\sqrt{y^2 + c^2}}. \tag{B-11}$$

This estimate is not valid for c = 0. For c = 0 we use the expression (45)

$$\hat{\mathcal{G}}_0(y, c, s)$$

$$= -2\left(\frac{y}{2}\right)^{i2\pi s} \frac{\Gamma(1 - i\pi s)}{\Gamma(1 + i\pi s)} {}_2F_1\left(-i\pi s, -\frac{1}{2}; \frac{1}{2} \left| -\frac{c^2}{y^2}\right.\right), \tag{B-12}$$

and we find

$$|\hat{\mathcal{G}}_0(y, 0, s)|$$

$$= \left| -2 \left(\frac{y}{2}\right)^{i2\pi s} \frac{\Gamma(1 - i\pi s)}{\Gamma(1 + i\pi s)} {}_2F_1\left(-i\pi s, -\frac{2}{2}; \frac{2}{2}; 0\right) \right| = 2.$$

$$(B-13)$$

On the axis, $y = 0$, we have equation (54)

$$\hat{\mathcal{G}}_0(c, s) = \left(\frac{c}{2}\right)^{i2\pi s} \frac{1}{i2\pi s - 1} \frac{\Gamma(1 - i\pi s)}{\Gamma(1 + i\pi s)} \quad (B-14)$$

and thereby

$$|\hat{\mathcal{G}}_0(c, s)| = \left| \frac{1}{i2\pi s - 1} \right| < 1. \quad (B-15)$$

Recollecting the results, we have found for the E-field filters

$$|\hat{G}_0(y, c, s)| \le \frac{\pi}{y} \sqrt{|s|} + \frac{1}{|c|} \quad y \ne 0, \, c \ne 0, \quad (B-16)$$

$$|\hat{G}_0(y, c, s)| = 0 \quad y \ne 0, \quad c = 0, \quad (B-17)$$

and

$$|\hat{G}_0(y, c, s)| \le \frac{1}{|c|} \quad y = 0. \quad (B-18)$$

For potential difference filters we find

$$|\hat{\mathcal{G}}_0(y, c, s)| \le \frac{2\pi|c|}{y} \sqrt{|s|}$$

$$+ 2 \frac{\sqrt{y^2 + c^2}}{v} \text{Artanh} \frac{y}{\sqrt{y^2 + c^2}} \quad y \ne 0, \, c \ne 0,$$

$$(B-19)$$

$$|\hat{\mathcal{G}}_0(y, c, s)| = 2 \quad y \ne 0, \quad c = 0, \quad (B-20)$$

and

$$|\hat{\mathcal{G}}_0(y, c, s)| \le 1 \quad y = 0. \quad (B-21)$$

All terms independent of s present no difficulties, since the theory of fast Hankel transforms applies. The constants entering the expressions will typically be of the order of magnitude of 1 or smaller.

The term involving $\sqrt{|s|}$ can be dealt with if we can calculate the integral

$$E(\omega_0, a, s_c, \lambda) = \int_{-\infty}^{\infty} |s|^\lambda \exp(-2\pi\omega_0|s|)[1$$

$$- \hat{P}(\Delta s)] \, ds. \quad (B-22)$$

The integral is convergent, since $0 < [1 - \hat{P}(\Delta s)] < 1$ and it can be expressed in terms of infinite sums of incomplete gamma functions. The case $\lambda = 1/2$, $\omega_0 = \pi/4$, which is the relevant one in this connection, has been integrated numerically for optimized filters with different s_c, and the result is shown in Figure B-l. The error expression plotted is normalized with respect to the error of fast Hankel transforms $E(\omega_0, a, s_c, \lambda = 0)$ given in Christensen (1990). We see a very moderate increase in the error with increasing cut-off frequency s_c compared with the results from the theory of optimized fast Hankel transforms.

For all practical purposes, as a rule of thumb, we may say that the computational error using the integrated Hankel filters is of the same order of magnitude as for ordinary Hankel filters.
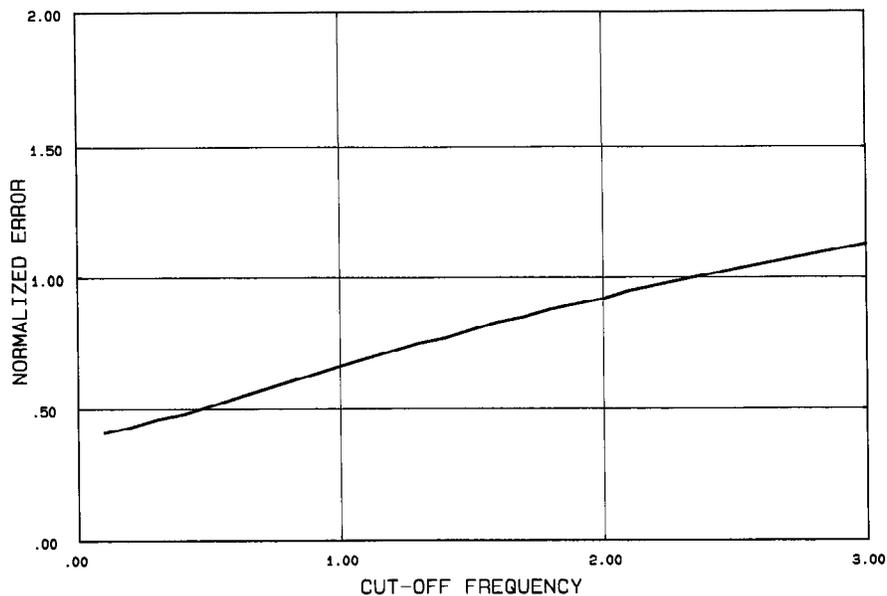

FIG. B-l. The error integral appearing in equation (B-22) of the integrated Hankel transform method as a function of the cut-off frequency s_c for $\lambda = 1/2$, $\omega_0 = \pi/4$. The error is normalized with respect to the error integral of ordinary optimized fast Hankel transforms.